

A Study of Seismic Noise Level at the KNET Stations

N. A. Sycheva^a, I. V. Sychev^b, A. N. Mansurov^a, and S. I. Kuzikov^{a, *}

^aResearch Station, Russian Academy of Sciences, Bishkek-49, 720049 Kyrgyzstan

^bTrofimuk Institute of Petroleum Geology and Geophysics (IPGG), Siberian Branch, Russian Academy of Sciences, prosp. Akademika Koptyuga, 3, Novosibirsk, 630090 Russia

*e-mail: ksi@gdirc.ru

Received September 21, 2019; revised September 21, 2019; accepted March 31, 2020

Abstract—We estimated the level of seismic noise for stations of the KyrgyzNetwork (KNET) for 19 years of its operation (1999–2017) in real time. For each channel of a seismic station (east–west, north–south, vertical) we selected fifteen-minute segments of 100-Hz seismic noise distributed over all seasons of the year (March, June, September, and December) and several times of the day (0, 6, 12, and 18 h UTC). We calculated power spectral densities of seismic noise and found the probability density of signal power spectral density for all selected frequencies/periods. The resulting distributions were compared with Peterson’s seismic noise models (Peterson, 1993). The maximum absence of stochastic noise occurred at 00 and 18 h UTC for all KNET stations. The level of seismic noise is little affected by the seasons at periods of 2–5 s, slightly lowering in the summer and increasing in the cold seasons at periods of 5–10 s. September is the less favorable for periods of 0.02–2 s. The stations as a whole possess good characteristics at periods of 0.02–10 s (frequencies of 0.1–50 Hz) and can well be said to be noiseless.

Keywords: KNET, station, channel, seismic records, seismic noise, power spectral density

DOI: 10.1134/S0742046320040065

INTRODUCTION

The Kyrgyz seismological network, KNET (KyrgyzNet), was installed in August–September 1991 by coordinated effort of several organizations, viz., the Institute of Geophysics and Planetary Physics, University California San Diego (IGPP-UCSD), the Kyrgyz Institute of Seismology (KIS), the Institute for High Temperatures of the Russian Academy of Sciences (IHT RAS), the Institute of Physics of the Earth RAS (IPE RAS), and the Indiana State University (ISU). At the time the KNET was set up, it was one of the more advanced networks worldwide. Ten stations were equipped with broadband seismometers. These included 16-bit digital converters which encompass 90 dB of recorded dynamic range. One important advantage of this network consists in the fact that all seismographs are installed on bedrock, providing for a minimum of noise.

Prior to 1991, most seismic stations in Central Asia used analog instruments with limited frequency response functions. This was only sufficient for few problems to deal with, viz., event location, earthquake catalogs, focal mechanisms of earthquakes, and other problems that do not require advanced technologies. The installation of digital KNET seismographs of the new generation yielded data with a higher resolution that were amenable to high technology processing.

Six KNET stations surround the capital of Kyrgyzstan, Bishkek, and stand along the edges of the Chu valley (Fig. 1). The three stations in the northern row are situated along the northeastern boundary of the Chu Basin.

The intermediate along-latitude row of three seismic stations lies along the northern spurs of the Kirgiz mountain range. Lastly, the four stations in the southernmost row cover the area from the Susamy Basin to the southwestern circumference of the Issyk-Kul Depression. The naming of each station was governed by its proximity to a population center in Kyrgyzstan or Kazakhstan. Table 1 lists code names and geographic characteristics of the KNET seismic stations.

According to the general map (see Fig. 1), the USP, CHM, and TKM2 stations make a northern row of the observing network along the junction zone between the Chuya Depression and the foothills of the mountains further northeast. Viewed on a larger scale, the topographic situation reduces to comparatively gently sloping relief forms with erosional incisions of a few tens of meters and altitudes of 650–2000 m (Fig. 2, top row). The areas around the stations are mostly composed of Quaternary terrigenous deposits with windows where bedrocks of the Paleozoic basement are exposed.

The next row consists of the EKS2, AAK, and KBK stations (see Fig. 2, second row from above), it is

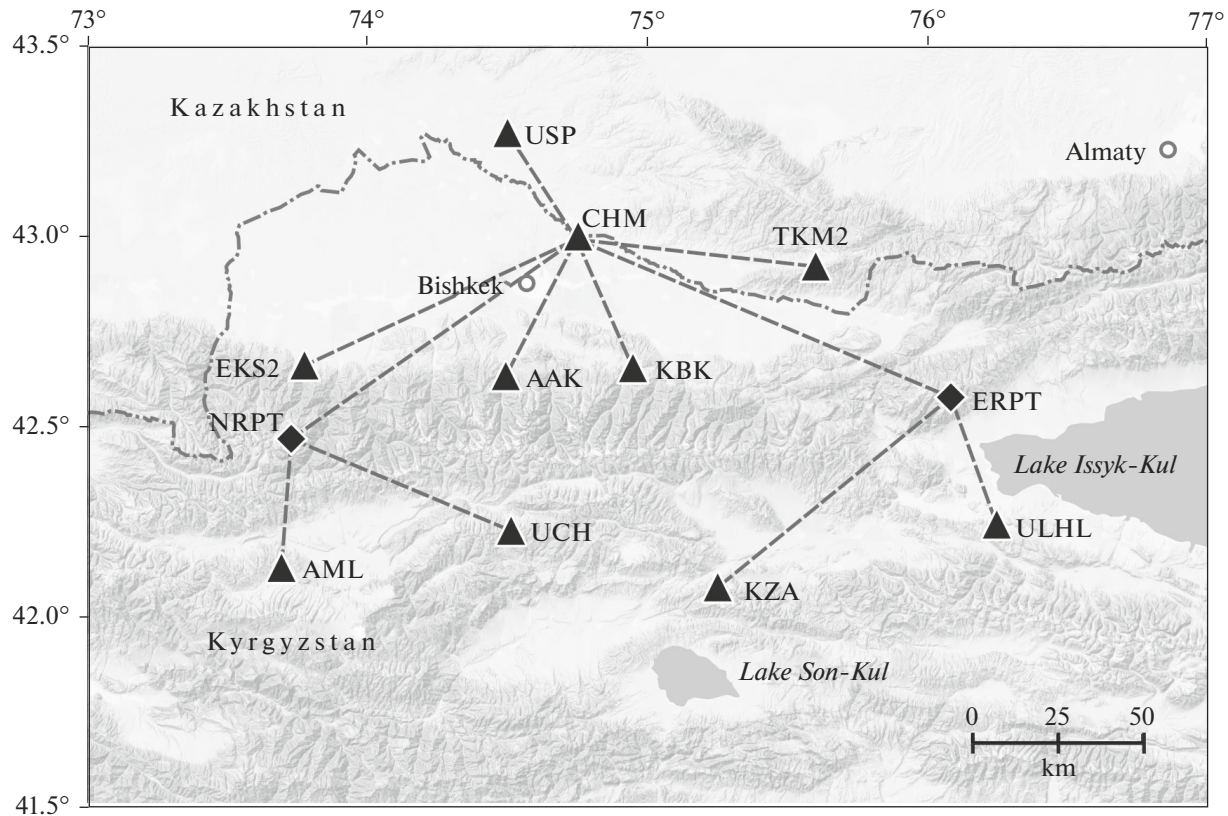


Fig. 1. Stations of the Kyrgyz seismological network (KNET). Triangles mark the seismic stations; dashed lines represent radio telemetry communication between the stations and repeaters (quadrangles) for control and data transmission.

in the foothills between the Chu Valley and the northern slopes of the Kirgiz Range. The altitudes north of these stations are 1350–1800 m; the relief becomes flatter, while south of the stations we have an increasing gradient of elevation and increasing incision by water streams. Characteristically, this zone is a junction area between Paleogene-Neogene poorly lithified deposits (from the north) and Paleozoic bedrock features (mostly granites, from the south).

The southwestern part of the KNET area contains the AML and UCH stations, as well as the NRPT repeater to ensure telecommunication with the Chu Basin (see Fig. 1). This set of facilities has the greatest altitude range, 3400–4250 m (see Fig. 2, second row from below), containing the divide areas of the Kirgiz, Suusamy, and Jungaltau mountain ranges. Here one can see an exposed stratified Paleozoic crystalline basement having considerable seismic activity (the 1992 Suusamy earthquake with M_S 7.4) and traces of recent tectonic activity (faults, slickensides, rock cracking).

Last, the southeastern part of the KNET network contains the KZA and ULHL stations, as well as the East repeater that connects them (ERPT). These facilities are situated in the area between the Kyzart Mountains and the western termination of the Kungei

and Terskei mountain ranges. The altitude range is considerable, 2050 to 3750 m (see Fig. 2, bottom row), the gradient of topographic dissection is high. The rocks are mostly Paleozoic bedrock exposures, while Paleogene-Neogene deposits are less abundant. The stations in the area are usually characterized as “noisy” because of considerable microseismic background noise of unidentified origin.

The network stations have STS-2 seismometers, which generate output voltages that are proportional to ground velocity and have a transfer function that is constant over a wide frequency range, between 0.01 and 10 Hz. In the range from 10 to 40 Hz the seismograph amplifies the record and introduces a phase shift, which can be corrected for by subsequent processing. (<https://www.passcal.nmt.edu/content/instrumentation/sensors/broadband-sensors/sts-2-bb-sensor>).

Seismic noise consists of very weak oscillations (microseisms) resulting from diverse sources like wind, water waves in water bodies, or waves striking the shore. Some of these are excited by standing waves in seas and oceans during the passage of cyclones, etc. Microseisms are recorded in a wide frequency range, and make a natural background that controls the sensitivity threshold for seismographs. A low noise level in

Table 1. The geographic characteristics of KNET stations and repeaters

| | | | | | | |
|----|------|----------------|---------|---------|------|--|
| 1 | AAK | Ala-Archa | 42.6333 | 74.4944 | 1680 | Ala-Archa Valley, village of Kashkasu, Kyrgyzstan |
| 2 | AML | Almaly-Ashuu | 42.1311 | 73.6941 | 3400 | Almaly-Ashuu Pass, Kyrgyzstan |
| 3 | CHM | Chumysh | 42.9986 | 74.7513 | 655 | Village of Chumysh, Chumysh Mountains, Kazakhstan |
| 4 | EKS2 | Erkin-Sai | 42.6615 | 73.7772 | 1360 | Village of Erkin-Sai, Kara-Bulak, Kyrgyzstan |
| 5 | KBK | Karagai-Bulak | 42.6564 | 74.9478 | 1760 | Village of Karagai-Bulak, Kyrgyzstan |
| 6 | KZA | Kyzart | 42.0778 | 75.2496 | 3520 | Kyzart Pass, Kyzart Mountains, Kyrgyzstan |
| 7 | TKM2 | Tokmak | 42.9208 | 75.5966 | 2020 | North slope of Kastek Range, Kazakhstan, 30 km from the town of Tokmak, Kyrgyzstan |
| 8 | UCH | Uch-Ter | 42.2275 | 74.5134 | 3850 | Uch-Ter Pass, Tyuz-Ashuu Pass, Kyrgyzstan |
| 9 | ULHL | Ulakhhol | 42.2456 | 76.2417 | 2040 | Village of Ulakhhol, Donuskuduk Tract, Kyrgyzstan |
| 10 | USP | Ezh-Uspenovka | 43.2669 | 74.4997 | 740 | Village of Betkainar (formerly Uspenovka), Kazakhstan |
| 11 | ERPT | East repeater | 42.5778 | 76.0778 | 3746 | Kalmak-Ashuu Pass, Kungei Alatau Range, Kyrgyzstan |
| 12 | NRPT | North repeater | 42.4694 | 73.7278 | 4214 | Mazar-Ashuu Pass, Kirgiz Range, Kyrgyzstan |

φ is latitude, λ is longitude, H is altitude above sea level. The table does not provide information for stations that were operated a short time, BLG (Belogorka) and TKM (Tokmak).

seismographs allows one to better locate weak seismic events and microseisms.

The first estimate of seismic noise level was made in a study of relationships between noise level and solar flare (Sycheva et al., 2011). This required assessment of the noise itself. We analyzed the rms deviation of 900-second segments of seismic signals at the AAK station during summer and winter months lasting 60 days (Fig. 3). The mean level of the rms deviation during the summer months was below that recorded during the winter months: while the level varied around 0.2×10^4 nm/s in the summertime, it reached 1.5×10^4 nm/s in the wintertime. The winter months also showed some quasi-periodicity and larger changes in the rms deviation.

Sycheva and Mansurov (2018) calculated station corrections (site-effect) for the KNET stations using records of seismic noise following the method of Nakamura (1989). For high-altitude stations, which are south of the axis of the Kirgiz Range (AML, UCH, and KZA), we obtained several frequently encountered variants of deviations in the spectral ratio of horizontal to vertical component (H/V) compared with the value that is typical of the station. This might happen because of considerable increase or decrease in noise level for a channel, which could have resulted from climatic variations.

THE DATA SET AND THE METHOD

Beginning July 1998, the KNET stations have been operated in real time, yielding continuous data, nearly all of the data (98–99%). We studied the level of seismic noise at the KNET stations by using digital records at 100 Hz sample rate for the period from the beginning of 1999 to mid-2017. The continuous records were used to make seismic noise segments

15 min long (900 s). The segments were selected from four time intervals over 24 h at a step of 6 hours: 00, 06, 12, and 18 hours UTC. The time intervals were selected from four months over the different seasons of the year (March, June, September, and December) for each year under consideration. These months were chosen as the months of the spring and autumn equinoxes and the months of the longest and the shortest night. An analysis of segments of seismic noise was to determine whether the noise level was affected by the season, the time of the day, and whether it varies from year to year. The resulting data set consisted of ~240000 segments of seismic noise. Of this number, only those segments with no seismic events and impulsive noise were used.

The frequency content of seismic noise was studied by finding probability power spectral density (PPSD) of seismic noise for all three measured components (E, N, Z). The procedure (McNamara and Buland, 2004) is as follows.

1. For each seismometer at a station we made sets (samples) of seismic noise segments (examples of the sets: records for a specified year, for a specified hour, all records).
2. Each segment was processed to find power spectral density (PSD), and velocities as measured by the seismometer were converted to accelerations in the frequency domain. Traditionally, PSD as a function of frequency is replaced with PSD as a function of period.
3. For the entire set of segments we chose discrete periods at a step of 1/8 octaves, and the PSD for each segment was rediscrretized with smoothing to these values of period.
4. For the entire data set the range of PSD values was also subdivided into subranges one dB wide each. A PPSD matrix was constructed where each column

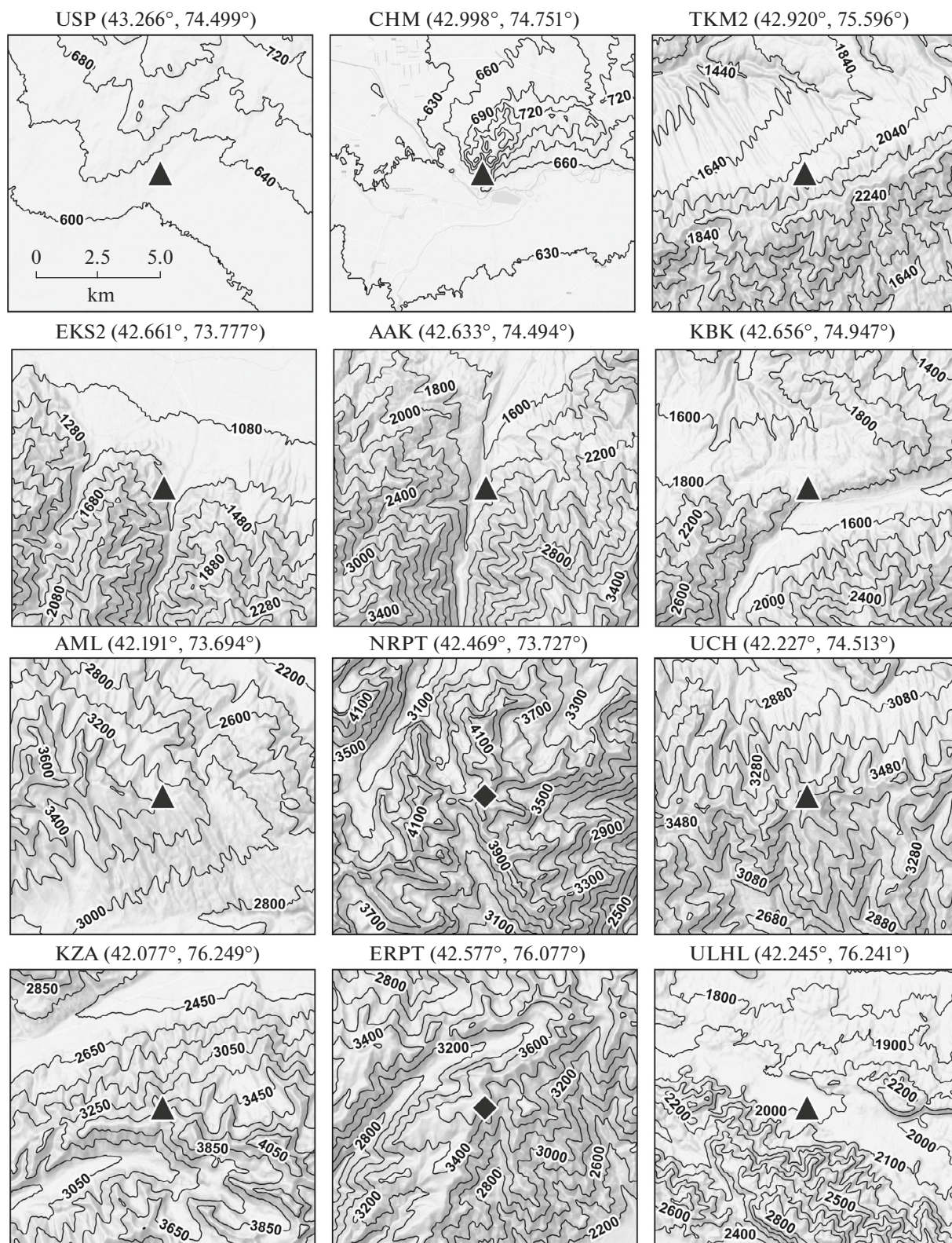


Fig. 2. Areas of a topographic map (0.1° latitude by 0.15° longitude). In the centers are KNET stations and repeaters, captions giving station code and the coordinates (N, E).

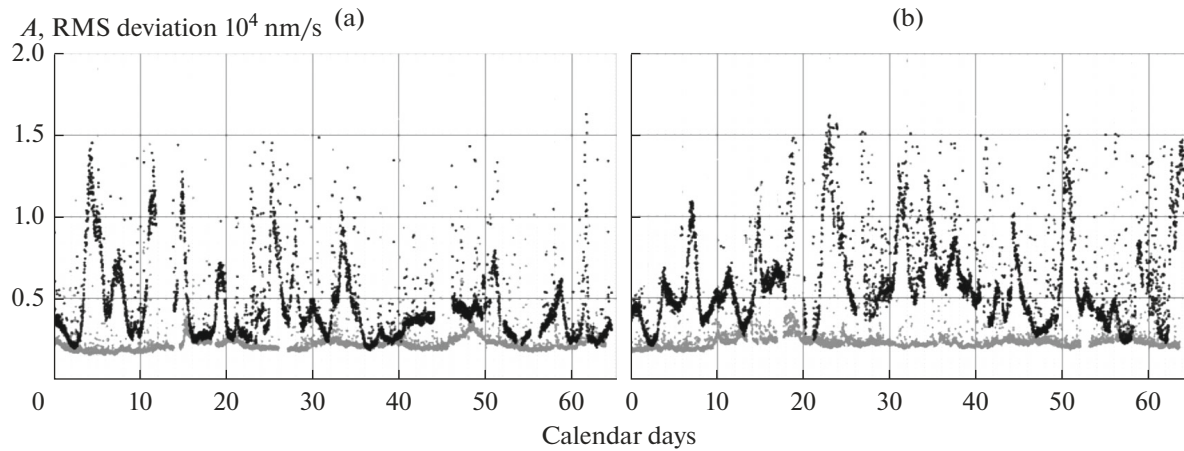


Fig. 3. The variation in the noise RMS error at the Alla-Archa station (AAK) during the months of summer (grey) and winter (black): (a) May 22, 2003 to July 22, 2003, November 22, 2003 to January 22, 2004; (b) May 22, 2004 to July 22, 2004, November 22, 2004 to January 22, 2005 (Sycheva et al., 2011).

corresponded to a period and each row to a PSD sub-range. The value of an element in the matrix was found as the relative number of segments in the data set under examination for which the PSD value at the corresponding period fell into the corresponding sub-range.

5. The resulting PPSD matrices were visualized as heatmaps.

Each segment leaves a “trace” in a PPSD heatmap as the pixel plot of its PSD. The more segments are in the heatmap, the “paler” is the trace left by each individual segment, but the PSD values may happen to be similar at some frequencies and to fall into the same range; in that case their “traces” are summed up and become brighter. Each column in a PPSD matrix is the probability power density; hence, one can find the mean of the density and plot the PSD mean against frequency.

We used our own software with some additional libraries to make segments of seismic noise, to plot the waveforms, to inspect the data, and to construct the PPSD. We dealt with data in the miniSEED format using the *obspy* library (A Python Toolbox for seismology/seismological observatories, <https://docs.obspy.org/>). As well, we used the PPSD class from the same library for automatic calculation and visualization of PPSD matrices. It is pointed out in the documentation to this library that the algorithms for PPSD calculation are based on the method of McNamara and Buland (2004). Information on the standard model of high and low noise level was taken from (Peterson, 1993) where these were denoted *NHNM* and *NLNM*, respectively; our notation in this paper employs *HiMdl* and *LoMdl*.

Processing for each channel (E, N, Z) resulted in PPSD of seismic noise for the following data sets.

For the entire period of study (1999–2017).

For the entire period of study at four times of the day (00, 06, 12, and 18 h, UTC).

For the entire period of study, during four months (March, June, September, and December).

For each year of study.

For each year and for four months (March, June, September, and December).

RESULTS AND DISCUSSION

Results for the entire period of study

The number of segments (n) taken up for processing from the entire data set and the dates of the first and last segments for each station are listed in Table 2. A total of ~50000 seismic noise segments was used, with the mean number of segments for each channel of all network stations being ~16500. For each station we processed approximately equal numbers of records for each channel. The maximum number of segments was for the UCH station ($n = \sim 2260$ for each channel) and for AAK ($n = \sim 2130$ for each channel), the minimum number was at the KBK station ($n = \sim 740$ for each station). Inspection of the KBK noise segments revealed frequent occurrences of high-amplitude signals of unknown origin (not earthquakes), while there being no such phenomena at the other stations; these records have been excluded from analysis.

Heatmaps showing the power spectral density of seismic noise as recorded by each channel of a station relative to the models of Peterson (1993) are shown in Figs. 4 and 5. These heatmaps can be used to estimate the position of the maximum PPSD curve relative to model curves at different periods in the spectrum, as well as to assess the scatter of power values within the sample at different frequencies. The position of the PPSD maximum relative to the models tells us something about the noise level at the respective station,

Table 2. The period and the number of processed segments of seismic noise for each channel of the KNET stations

| Number of segments | Channel | Stations | | | | | | | | | |
|--------------------|---------|----------|------|------|------|-----|------|------|------|------|------|
| | | AAK | AML | CHM | EKS2 | KBK | KZA | TKM2 | UCH | ULHL | USP |
| | E | 2134 | 1475 | 1915 | 1544 | 735 | 1397 | 1223 | 2354 | 1836 | 1917 |
| | N | 2133 | 1475 | 1910 | 1547 | 735 | 1395 | 1218 | 2357 | 1836 | 1927 |
| | Z | 2133 | 1474 | 1914 | 1548 | 736 | 1394 | 1215 | 2358 | 1836 | 1920 |

The starting date for each station is March 1, 1999; the end date is June 30, 2017 for AAK, AML, CHM, TKM2, and USP; September 29, 2015 for KZA; June 28, 2017 for KBK; June 29, 2017 for UCH and ULHL; and June 14, 2017 for EKS.

Table 3. The position of the PPSD maximum relative to the model curves at different periods on the three channels (E, N, Z) of the KNET stations

| Channel | E | | | | N | | | | Z | | | |
|---------|---------------------|-----|------|--------|---------------------|-----|------|--------|---------------------|-----|------|--------|
| Station | Range of periods, s | | | | Range of periods, s | | | | Range of periods, s | | | |
| | 0.02–2 | 2–5 | 5–10 | 10–100 | 0.02–2 | 2–5 | 5–10 | 10–100 | 0.02–2 | 2–5 | 5–10 | 10–100 |
| AAK | L~M | L~ | L~ | M~H | L~M | L~ | L~ | M~H | L~M | L~ | L~ | L~ |
| AML | L~M | L~ | L~ | M~H | L~M | L~ | L~ | M~H | L~M | L~ | L~ | L~ |
| CHM | L~M | L~ | L~ | H< | L~M | L~ | L~ | H< | L~M | L~ | L~ | L~ |
| EKS2 | L~M | L~ | L~ | H< | L~M | L~ | L~ | H< | L~M | L~ | L~ | L~ |
| KBK | L~M | L~ | L~ | ~H | L~M | L~ | L~ | H< | L~M | L~ | L~ | L~ |
| KZA | L~M | L~ | L~ | ~H | L~M | L~ | L~ | ~H | L~M | L~ | L~ | L~ |
| TKM2 | L~M | L~ | L~ | M~H | L~M | L~ | L~ | M~H | L~M | L~ | L~ | L~ |
| UCH | L~M | L~ | L~ | ~H | L~M | L~ | L~ | ~H | L~M | L~ | L~ | L~ |
| ULHL | L~M | L~ | L~ | ~H | L~M | L~ | L~ | ~H | L~M | L~ | L~ | L~ |
| USP | L~M | L~ | L~ | ~H | L~M | L~ | L~ | H< | L~M | L~ | L~ | L~ |

while the power scatter provides evidence of station stability.

The position of the PPSD maximum relative to the models varies in relation to the period (see Figs. 4, 5). The resulting spectra were examined in four ranges of period: 0.02–1, 1–5, 5–10, and 10–100 s. Depending on the position of the PPSD maximum relative to the models, we adopted the following notation in each range: L~ (close to the low-noise *LoMdl* model), ~H (close to the high-noise *HiMdl* model), L ~ M (below the middle point between the models), M ~ H (above the middle point between the models), H< (above *HiMdl*). According to this notation, Table 3 contains information on deviations from the models in the ranges of period considered here for each channel of each station. The lighter the color of a cell in this table, the closer is the PPSD maximum to the lower model (low noise).

An analysis of Table 3 and Figs. 4 and 5 showed that the vertical channel is the best: the PSD maximum for all network stations is below the middle point between the models (L~M) at periods below 1 s, and is close to the lower model at the other periods (L~).

The range 0.02–2 s. The position of the PPSD maximum for all stations in this part of the spectrum is below the middle point between the two models (L ~ M). The maxima are the closest to *LoMdl* for the AAK, AML, EKS2, KZA, UCH, and USP stations.

The range 2–5 s. The position of the PPSD maximum in this part of the spectrum is identical with the lower model or lies slightly above it for all stations. That means that the stations have the lowest noise level at these periods.

The range 5–10 s. In this range, the PPSD maxima for all stations are slightly above the lower model as well, which also means the minimum noise level.

The range 10–100 s. The positions of the PPSD maximum at these periods are discrepant, both between the channels and between the stations. As pointed out above, the PPSD maximum is slightly above the lower model for the vertical channels. The PPSD maxima of the horizontal channels at the AAK, AML, and TKM2 stations lie slightly above the middle point between the two models, are just adjacent to the upper model for KZA, UCH and ULHL, and even

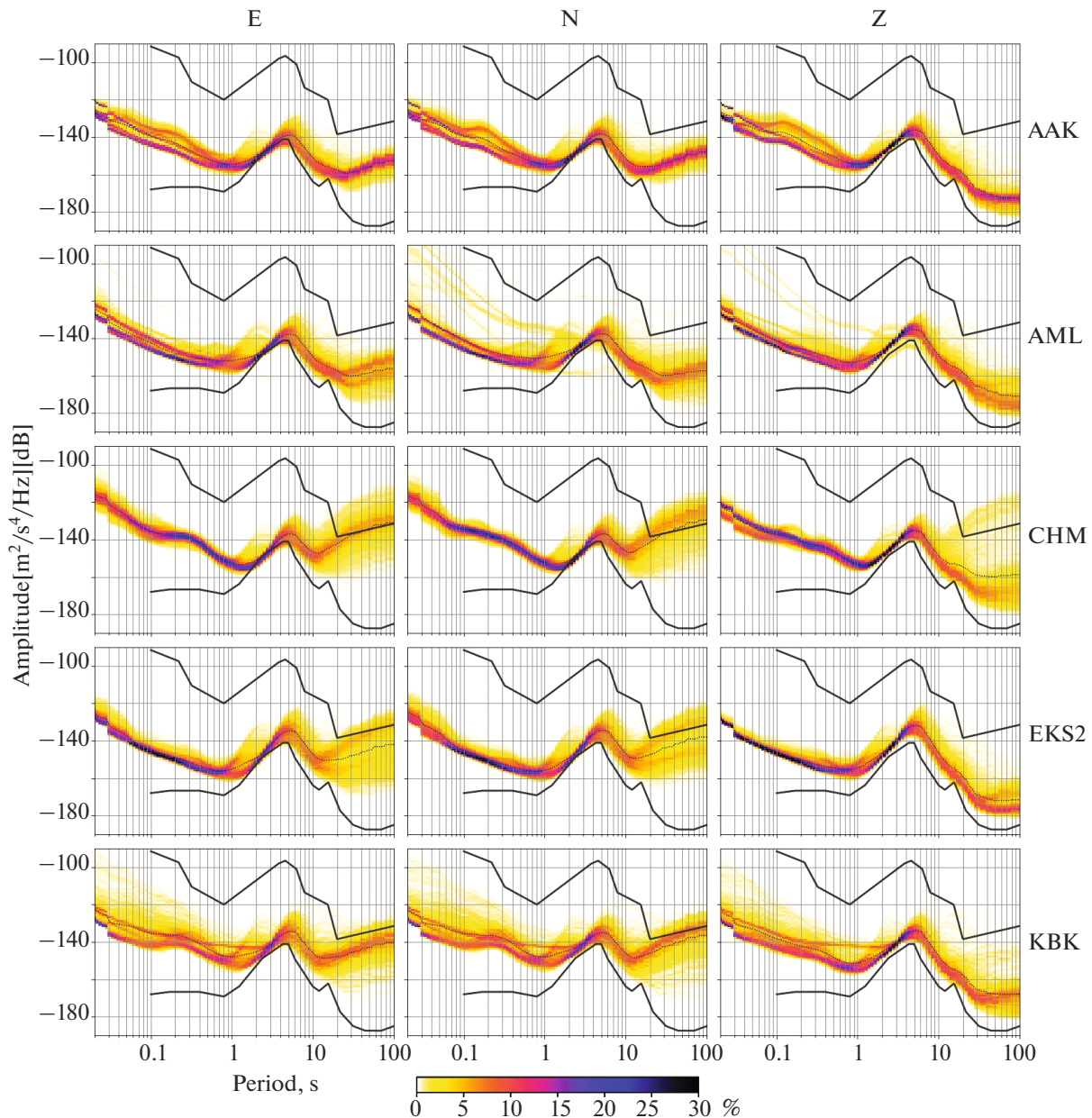


Fig. 4. The noise PPSD for all channels at the AAK, AML, CHM, EKS2, and KBK stations based on the entire data set. The black, thin, dashed line in this and subsequent figures represents the mean PSD as a function of frequency.

exceed the level of the upper model for CHM, EKS2, KBK, and USP.

The power scatter within the sample. Because the data set is so large, we have to introduce some summary estimate that one could label “quality”. Ascribing an estimate (I, II, or III) can depend both on the scatter among the spectra of individual noise segments (the larger the scatter, the lower is the quality) and on the upward displacement of the PPSD maximum relative to the lower model (the closer to the lower model, the higher is the quality).

It can be seen from Figs. 4 and 5 that the power scatter within the sample varies in relation to the period under consideration. Table 4 presents the results from an analysis of the distribution density (variance) in the different ranges of period using the estimates described above (I—denotes the minimum scatter among the spectra of individual noise segments; II—denotes the presence of a some low variance; III—means a large variance).

Good consistency among the spectra of individual segments at all periods is more frequently achieved for the Z channel (for I by a factor of 24, for II by a factor

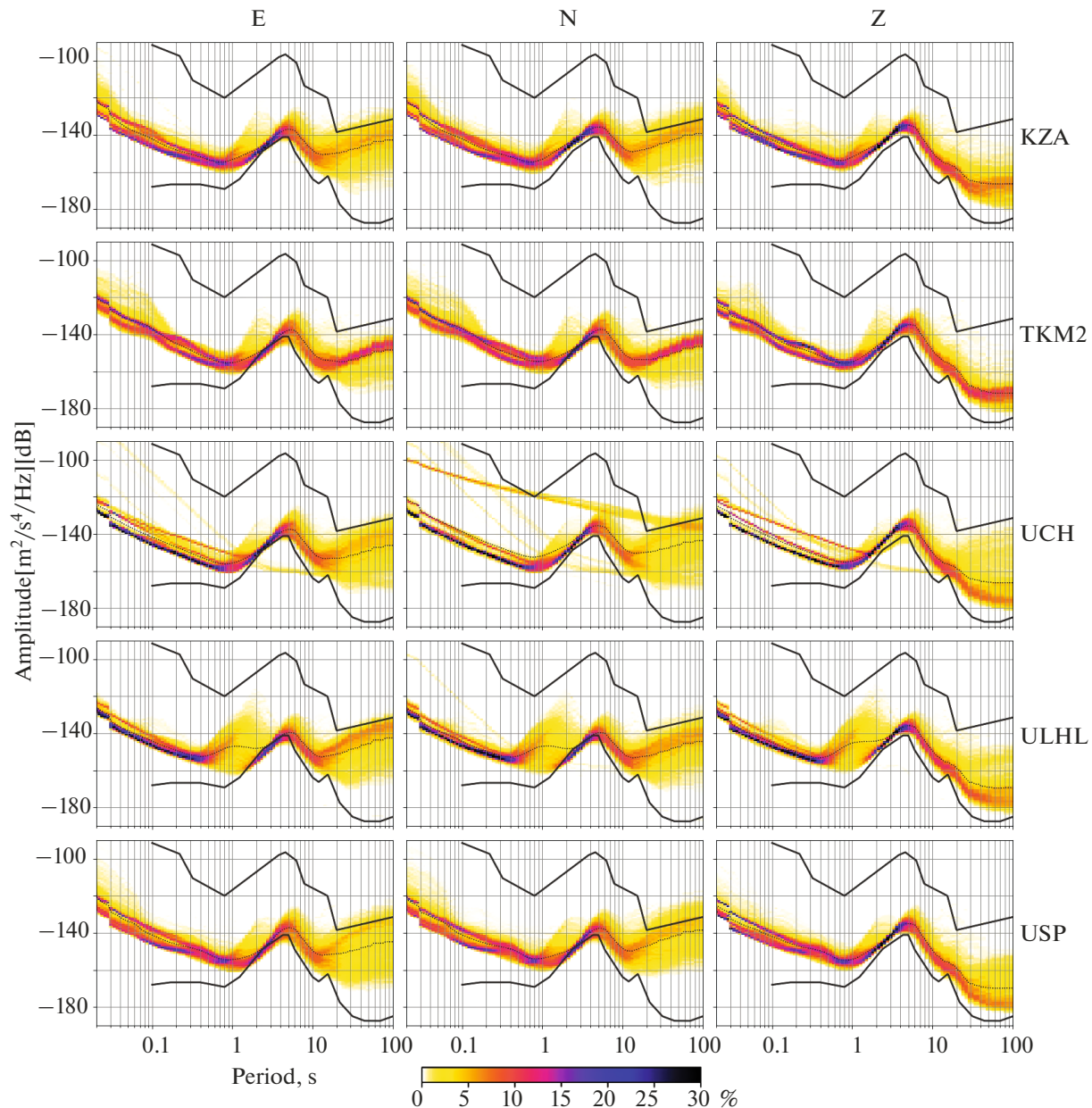


Fig. 5. The seismic noise PSD for all channels at the KZA, TKM2, UCH, ULHL, and USP stations based on the entire data set.

of 8, and for III by a factor of 8). The largest number of estimates of I for all channels was observed at CHM, AAK, and TKM2 (9, 8, and 8) and the least at KBK and ULHL (1, 1). The maximum number of estimates of I was at UCH and KBK (8, 4) and no such estimates were found at AAK and TKM2. The spectral scatter at AML and UCH was rather due to some individual considerable departures from the typical power spectrum.

The range 0.02–2 s. The considerable scatter between the spectra of different segments was observed at AML, UCH, and KBK. The other stations showed good consistency or a small variance.

The range 2–5 s. For these periods, small variances were observed at AML, KBK, and ULHL on all channels, while large variances occurred at the N channel of the UCH station.

The range 5–10 s. For this range some insignificant scatter between the spectra was observed at the N channels of EKS2, KBK, KZA, ULHL, and USP; a large variance occurred at the N channel of the UCH station.

The range 10–100 s. The variances are large on all channels of all stations, with considerable deviations between individual spectra being observed at CHM, EKS2, KZA, UCH, ULHL, and USP.

Table 4. The scatter of power within the sample at different periods at the KNET stations

| Channel | E | | | | N | | | | Z | | | |
|---------|--------------------|-----|------|--------|--------------------|-----|------|--------|--------------------|-----|------|--------|
| Station | Range of period, s | | | | Range of period, s | | | | Range of period, s | | | |
| | 0.02–2 | 2–5 | 5–10 | 10–100 | 0.02–2 | 2–5 | 5–10 | 10–100 | 0.02–2 | 2–5 | 5–10 | 10–100 |
| AAK | II | I | II | I | II | I | I | I | II | I | I | I |
| AML | II | II | I | II | III | II | I | II | III | I | I | II |
| CHM | I | I | I | III | I | I | I | III | I | I | I | III |
| EKS2 | I | I | II | III | I | I | II | III | I | I | I | II |
| KBK | III | II | II | II | III | II | II | II | III | II | I | III |
| KZA | II | I | II | III | I | I | II | III | I | I | I | II |
| TKM2 | I | I | I | I | II | I | II | II | II | I | I | I |
| UCH | III | I | I | III | III | III | III | III | III | I | I | III |
| ULHL | II | II | II | III | II | II | II | III | II | II | I | III |
| USP | II | I | II | III | II | I | II | III | I | I | I | III |

I—good agreement between the spectra of individual segments; II—there is a small variance; III—a large variance.

The Results for the Entire Period of Study During the Four Times of the Day

Table 5 lists the number of noise segments processed for times of the day (00, 06, 12, and 18 h UTC) on each channel of the KNET stations: the greatest number of segments was for the UCH station (8110) and for AAK (7367), the minimum number for KBK (2672). The number of processed segments occurring at the times of the day (UTC) are 26 476 for 00 h, 6590 for 06 h, 6402 for 12 h, and 10124 for 18 h. These figures provide indirect evidence that the seismic noise around 00 and 18 h UTC is free of impulsive interference.

An analysis of 120 heatmaps (10 stations, 3 channels, 4 times of the day) showed that the position of the PPSD maximum is practically independent of the time of the day. We therefore believe that the quality estimate was largely affected by the scatter among the spectra of individual segments at different periods (variance). The results of the PPSD analysis using the abovementioned quality estimates are listed in Table 6. We counted the estimates for all stations at a particular time of the day to get the following result: 00 hours UTC (I, 22 times; II, 7; and III, once), 06 hours (I, 7 times; II, 20; and III, 3 times), 12 hours (I, 10 times; II, 11; and III, 9), and 18 hours (I, 14 times; II, 9; and III, 7 times). These relationships among the estimates of I, II, and III for each time of the day show that 00 UTC is the best time for station operation. The largest variance in PPSD is observed at 12 UTC. The AAK and TKM2 stations are the least sensitive to changes in the time of the day, while the KBK station obviously possesses this sensitivity: the number of segments whose PPSD shows large departures from the curve of the PPSD maximum is the lowest in the nighttime and in the morning rather than in the daytime and in the evening.

Figure 6a shows the PPSD of two stations, AAK and EKS2, for different times of the day. The first of these stations is in an underground galley situated in the Ala-Archa ravine at an altitude of 1680 m, and the second is on the slope of a mountain at 1360 m altitude. The difference in the PPSD characteristic during different hours at AAK is nearly absent, while the level of seismic noise at EKS2 at periods longer than 10 s is affected by the time of the day. In the daytime one sees the variance increasing between the spectra of different segments.

The Results for the Entire Period of Study in Relation to Seasons of the Year

The numbers of noise segments as processed for the months of March, June, September, and December for each channel are listed in Table 7: the greatest number was processed for the UCH station (7796) and for AAK (7041), and the minimum number for KBK (2487). The relationship among the numbers of processed segments for the seasons of the year is as follows: 16052 for March, 14081 for December, 10378 for June, and 9080 for September. These relationships may constitute indirect evidence that March is the best month for the stations and September the worst.

The distribution of seismic noise power was estimated separately for each of the following ranges: 0.02–2 s, 2–5 s, 5–10 s, and 10–100 s. Both the position of the PPSD maximum and the scatter among the spectra of individual segments vary in different ways in relation to the season within these ranges of period. The results from the inspection of the PPSD (120 heatmaps) are summarized in Table 8.

Table 9 presents a summary distribution of the estimates for each season under investigation and the range of period.

Table 5. The numbers of segments (n) with recorded seismic noise for the times of the day (00, 06, 12, and 18) at each channel of the KNET stations

| Channel | E | | | | N | | | | Z | | | |
|---------|-----------|-----|-----|-----|-----------|-----|-----|-----|-----------|-----|-----|-----|
| Station | UTC hours | | | | UTC hours | | | | UTC hours | | | |
| | 00 | 06 | 12 | 18 | 00 | 06 | 12 | 18 | 00 | 06 | 12 | 18 |
| AAK | 968 | 313 | 316 | 537 | 967 | 313 | 316 | 537 | 967 | 313 | 316 | 537 |
| AML | 721 | 242 | 224 | 288 | 721 | 242 | 224 | 288 | 721 | 242 | 224 | 287 |
| CHM | 1134 | 171 | 183 | 427 | 1132 | 171 | 182 | 425 | 1133 | 171 | 183 | 427 |
| EKS2 | 963 | 154 | 109 | 318 | 965 | 154 | 109 | 319 | 964 | 155 | 109 | 320 |
| KBK | 466 | 63 | 58 | 148 | 466 | 64 | 58 | 147 | 466 | 64 | 58 | 148 |
| KZA | 691 | 220 | 236 | 250 | 690 | 220 | 236 | 249 | 691 | 221 | 234 | 248 |
| TKM2 | 613 | 179 | 180 | 251 | 613 | 176 | 179 | 250 | 610 | 177 | 177 | 251 |
| UCH | 1039 | 422 | 397 | 496 | 1037 | 424 | 398 | 498 | 1040 | 422 | 398 | 499 |
| ULHL | 1098 | 228 | 238 | 271 | 1100 | 227 | 239 | 271 | 1100 | 227 | 239 | 270 |
| USP | 1129 | 205 | 194 | 389 | 1136 | 207 | 195 | 389 | 1135 | 203 | 193 | 389 |

Table 6. The PPSD “quality” for certain hours of the day (00, 06, 12, 18 UTC) at the KNET stations

| Channel | UTC hours | Stations | | | | | | | | | |
|---------|-----------|----------|-----|-----|------|-----|-----|------|-----|------|-----|
| | | AAK | AML | CHM | EKS2 | KBK | KZA | TKM2 | UCH | ULHL | USP |
| E | 00 | II | II | I | I | I | I | II | II | I | I |
| | 06 | I | I | III | II | II | I | I | II | II | II |
| | 12 | I | I | III | II | III | II | I | I | II | II |
| | 18 | I | II | II | I | III | II | II | II | III | I |
| N | 00 | II | I | I | I | I | I | II | III | I | I |
| | 06 | I | III | II | II | II | II | I | III | II | II |
| | 12 | I | III | II | III | III | II | I | III | II | I |
| | 18 | I | I | I | I | III | II | II | III | III | II |
| Z | 00 | II | I | I | I | I | I | I | I | I | I |
| | 06 | I | II | II | II | II | II | II | II | II | II |
| | 12 | I | II | II | III | III | II | I | I | III | II |
| | 18 | I | II | I | I | III | I | I | I | III | I |

According to this table, the range 5–10 s is the most sensitive to changes in the seasons of the year (high estimates were more numerous for the warmer season and less numerous for the cold), while the range 2–5 s is the least sensitive. For longer periods (10–100 s) one notices an instability in the level of seismic noise for all seasons of the year. September is the least favorable month at high frequencies (0.02–2 s).

If we exclude the long period motion (10–100 s), then all the stations can be treated as being stable under seasonal variations, except for KBK, AML, and UCH. March is the best season for TKM2 and AML, June for AAK, CHM, EKS2, USP, and KZA, Sep-

tember for CHM, and USP, and December for KBK, KZA, TKM2, UCH, and ULHL.

Figure 6b shows the PPSD for two stations over the seasons of the year (AAK and CHM). The AAK station is installed in the ravine at an altitude of 1680 m, and the CHM station on the slope of a low mountain (altitude 655 m). The quality of operation for the AAK station is little affected by seasonal variations, while CHM is season-sensitive at periods longer than 10 s. The variance of the distribution becomes greater at these periods during the cold seasons. Figure 7 shows the noise PPSD for March, June, September, and December for all channels at the KBK station. March and September are the best times for the station.

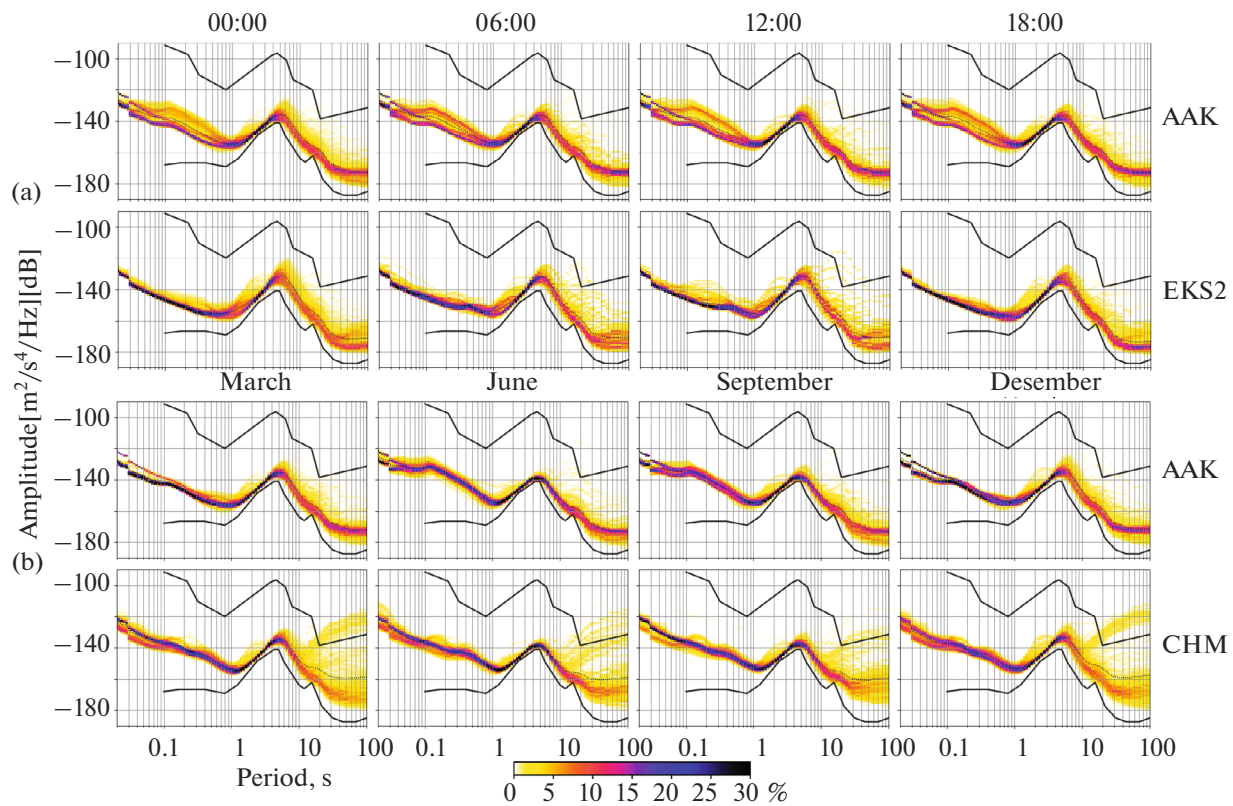


Fig. 6. The seismic noise PSD (Z channel): (a) over times of the day (AAK and EKS2); (b) over the seasons (AAK and CHM).

The ULHL station. Our study of the station PSD over times of the day and the seasons of the year revealed one peculiar feature of the ULHL station, which is situated on the southwestern shore of Lake Issyk-Kul. The seismic noise at the station shows an unstable behavior at periods of 0.5–3.5 s, whatever the season or the time of the day (Fig. 8).

The Results for Each Year of the Study (1999–2017)

Inspection of the noise PSD at the KNET stations for each year of study (570 heatmaps) showed that, in consideration of the shapes of the curves, these are little different from the PSD based on the entire data set. Overall, the operation of the KNET stations

Table 7. The numbers of noise segments processed for different seasons of the year (March, June, September, and December) for each channel at the KNET stations

| Channel | E | | | | N | | | | Z | | | |
|---------|------|------|-------|------|------|------|-------|------|------|------|-------|------|
| | Mar. | June | Sept. | Dec. | Mar. | June | Sept. | Dec. | Mar. | June | Sept. | Dec. |
| AAK | 641 | 506 | 435 | 552 | 641 | 505 | 435 | 552 | 641 | 505 | 435 | 552 |
| AML | 458 | 367 | 261 | 389 | 458 | 367 | 261 | 389 | 458 | 367 | 261 | 388 |
| CHM | 600 | 306 | 442 | 567 | 600 | 302 | 442 | 566 | 600 | 306 | 442 | 566 |
| EKS2 | 509 | 229 | 328 | 478 | 511 | 230 | 328 | 478 | 511 | 232 | 328 | 477 |
| KBK | 281 | 120 | 91 | 243 | 281 | 121 | 90 | 243 | 281 | 121 | 91 | 243 |
| KZA | 438 | 383 | 209 | 367 | 438 | 383 | 208 | 366 | 434 | 383 | 209 | 368 |
| TKM2 | 474 | 182 | 143 | 424 | 471 | 183 | 143 | 421 | 470 | 180 | 143 | 422 |
| UCH | 722 | 596 | 425 | 611 | 722 | 605 | 423 | 607 | 727 | 596 | 424 | 611 |
| ULHL | 571 | 431 | 351 | 482 | 572 | 432 | 351 | 482 | 571 | 431 | 352 | 482 |
| USP | 656 | 335 | 344 | 582 | 659 | 335 | 345 | 588 | 656 | 339 | 340 | 585 |

Table 8. The quality (I high, II medium, III low) for the PSD of seismic noise for the seasons of the year (March, June, September, and December) in different ranges of period

| Station | Channel | E | | | | N | | | | Z | | | |
|---------|-----------|--------------------|-----|------|--------|--------------------|-----|------|--------|--------------------|-----|------|--------|
| | Month | Range of period, s | | | | Range of period, s | | | | Range of period, s | | | |
| | | 0.02–2 | 2–5 | 5–10 | 10–100 | 0.02–2 | 2–5 | 5–10 | 10–100 | 0.02–2 | 2–5 | 5–10 | 10–100 |
| AAK | March | I | I | II | II | I | I | II | II | I | I | II | I |
| | June | II | I | I | I | II | I | I | I | II | I | I | II |
| | September | II | I | I | II | II | I | I | II | II | I | I | II |
| | December | I | I | II | I | I | I | II | II | I | I | II | II |
| AML | March | I | I | II | II | I | I | I | I | I | I | II | II |
| | June | II | I | I | I | III | II | I | III | II | II | I | II |
| | September | I | I | I | III | II | I | I | III | III | I | I | I |
| | December | I | I | II | II | I | I | II | II | I | I | II | I |
| CHM | March | I | I | II | II | I | I | II | III | I | I | II | III |
| | June | I | I | I | II | I | I | I | III | I | I | I | III |
| | September | I | I | I | III | I | I | I | III | I | I | I | II |
| | December | I | I | II | III | I | I | II | II | I | I | II | III |
| EKS2 | March | I | I | II | III | I | I | II | III | I | I | II | II |
| | June | I | I | I | II | I | I | I | II | I | I | I | I |
| | September | I | I | I | III | I | I | I | III | I | I | I | I |
| | December | I | I | II | II | I | I | II | II | I | I | II | II |
| KBK | March | III | II | II | II | III | II | II | II | II | II | II | II |
| | June | III | II | II | III | III | II | II | III | III | II | II | III |
| | September | III | II | II | III | III | II | II | III | III | I | II | II |
| | December | II | II | II | II | II | II | II | II | II | II | II | II |
| KZA | March | I | I | II | II | I | I | II | II | I | I | II | II |
| | June | I | I | I | III | I | I | I | II | I | I | I | II |
| | September | I | I | I | III | II | I | I | II | II | I | I | II |
| | December | I | I | II | II | I | I | II | II | I | I | I | I |
| TKM2 | March | I | I | II | I | I | I | II | I | I | I | I | I |
| | June | I | I | I | II | I | I | I | III | I | I | I | I |
| | September | I | II | I | II | I | I | I | III | I | I | II | II |
| | December | I | I | II | I | I | I | II | I | I | I | I | I |
| UCH | March | I | I | I | I | I | I | I | III | I | I | I | I |
| | June | I | I | I | III | I | I | I | III | I | I | I | I |
| | September | III | I | I | III | III | III | III | III | III | I | I | III |
| | December | I | I | I | I | I | I | I | I | I | I | I | II |
| ULHL | March | I | I | I | II | I | I | I | II | I | I | I | II |
| | June | I | I | I | II | I | I | I | III | I | I | I | I |
| | September | I | I | I | I | I | I | I | II | I | I | I | II |
| | December | I | I | I | I | I | I | I | I | I | I | I | III |
| USP | March | I | I | II | III | I | I | II | III | I | I | I | II |
| | June | I | I | I | III | I | I | I | III | I | I | I | I |
| | September | I | I | I | III | I | I | I | III | I | I | I | II |
| | December | I | I | II | II | I | I | II | II | I | I | II | II |

Table 9. The distribution of “quality” estimates for the ranges of period and seasons under study

| Month | Range of period (s) and “Quality” (I, II, III) | | | | | | | | | | | |
|-----------|--|----|-----|-----|----|-----|------|----|-----|--------|----|-----|
| | 0.02–2 | | | 2–5 | | | 5–10 | | | 10–100 | | |
| | I | II | III | I | II | III | I | II | III | I | II | III |
| March | 27 | 1 | 2 | 27 | 3 | 0 | 10 | 20 | 0 | 7 | 16 | 7 |
| June | 21 | 5 | 4 | 25 | 5 | 0 | 27 | 3 | 0 | 8 | 9 | 13 |
| September | 17 | 6 | 7 | 26 | 3 | 1 | 25 | 5 | 0 | 3 | 11 | 16 |
| December | 27 | 3 | 0 | 27 | 3 | 0 | 8 | 22 | 0 | 13 | 14 | 3 |

can be judged stable from year to year. Figure 9 shows the PPSDs based on the TKM2 records for each year of study (the N channel).

The Results for the Four Months of Each Year of Study

An analysis of the PPSD for the four seasons of each year as recorded by all stations revealed the most problematic stations mentioned above, namely, AML, KBK, KZA, and UCH. The PPSD for some days was greatly different from the typical one based on the entire data set. The UCH and AML stations were traditionally assumed to be “quiet” stations (low noise level). Our study shows that this hypothesis is only valid during a definite season of the year.

Examination of the heatmaps for the above stations based on data recorded during different seasons yielded results summarized in Table 10 where for each channel we marked those months of the years with great numbers of accumulated segments whose PSDs

show considerable departures from the curve of the PPSD maximum based on the entire period of study.

According to Table 10, the high altitude stations in the south (AML, KZA, UCH) showed seasonal patterns only during certain months of the year. The unstable behavior of the AML station in the month of June was probably due to water coming into the station vault as nearby glaciers started melting, while the KZA and UCH stations had their level of seismic noise affected by winds during the period from September to December. Figure 10 shows some examples of unstable behavior for these stations.

In March and June of 2009, the UCH station showed the usual stable level of seismic noise (see Table 10). In September one noticed an unusual behavior of the noise due to a failure at the station (a sensor malfunction). Figure 11 shows the PPSD at the UCH station for the four months of 2009; the failure might have occurred during period of July to Sep-

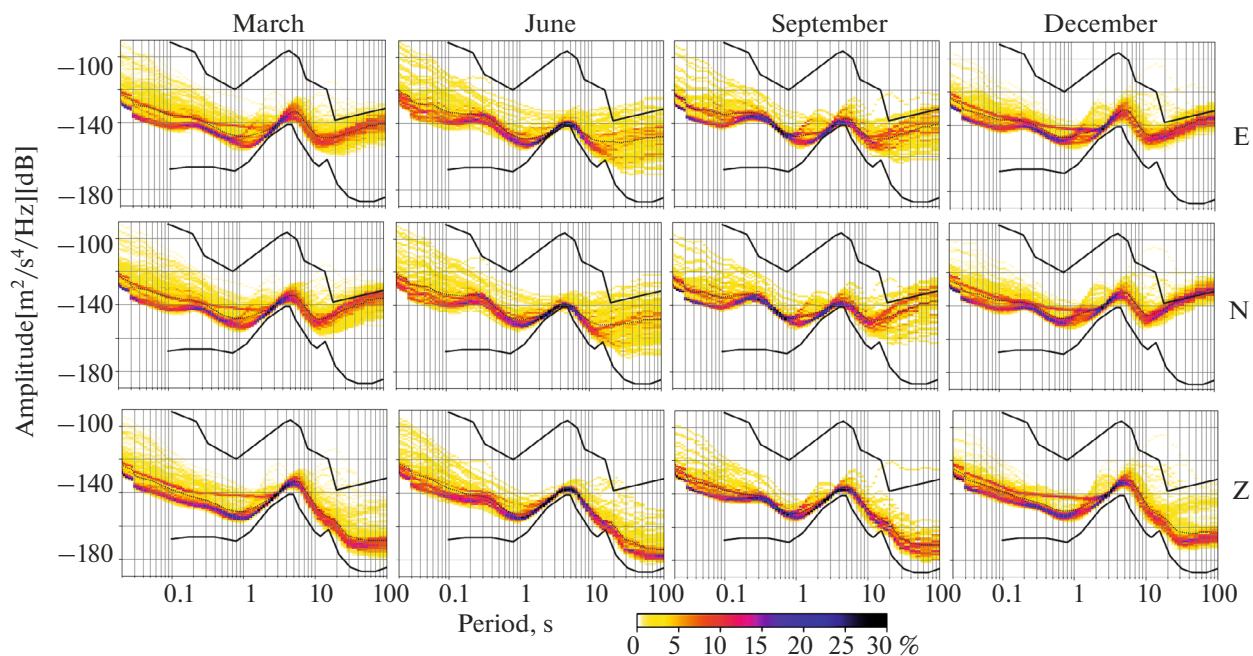


Fig. 7. The PPSD at the KBK station at all channels for March, June, September, and December.

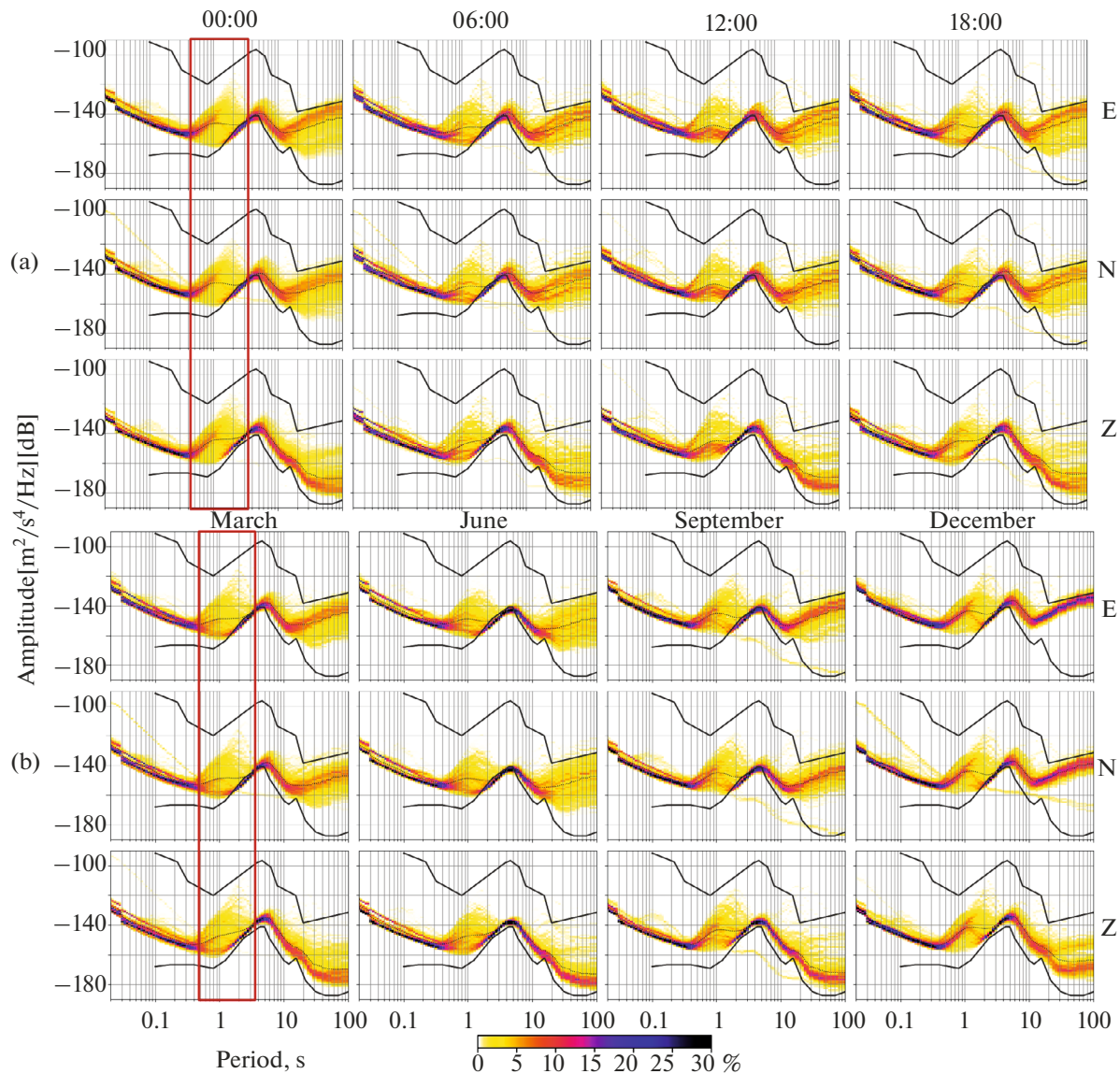


Fig. 8. The PPSD for the ULHL station over times of the day (a) and over the seasons (b) for all channels.

tember. The sensor was reinstalled and centered on November 24, 2009.

CONCLUSIONS

Our assessment of the quality of station operation in the KNET network was based on an analysis of over 50000 segments of seismic noise recorded in 1999 through 2017; each segment was 15 min long (900 s) and was observed during different times of the day (00, 06, 12, and 18 hours) and seasons of the year (March, June, September, and December) for all the three channels (E, N, Z). The level of seismic noise was estimated from the probability power spectral density (PPSD) of seismic signals with subsequent construction of heatmaps and comparison with the standard

models from (Peterson, 1993). This analysis of PPSDs has revealed the following.

1. The least deviation of the PPSD from the lower curve of the standard model (LoMdl or NLNM) at all stations was observed on the vertical channel (Z) at all periods.

2. Based on records for all channels, the curve of the PPSD maximum lies below the middle point between the lower model LoMdl and the upper model HiMdl for periods of 0.02–2 s and close to LoMdl for periods of 2–10 s. For the horizontal channels in the range of periods 10–100 s, large PPSD values correspond to powers much above the lower model, while even exceeding the upper model at some stations. When dealing with problems of local seismicity (the study of source spectra), the long period (10–100 s)

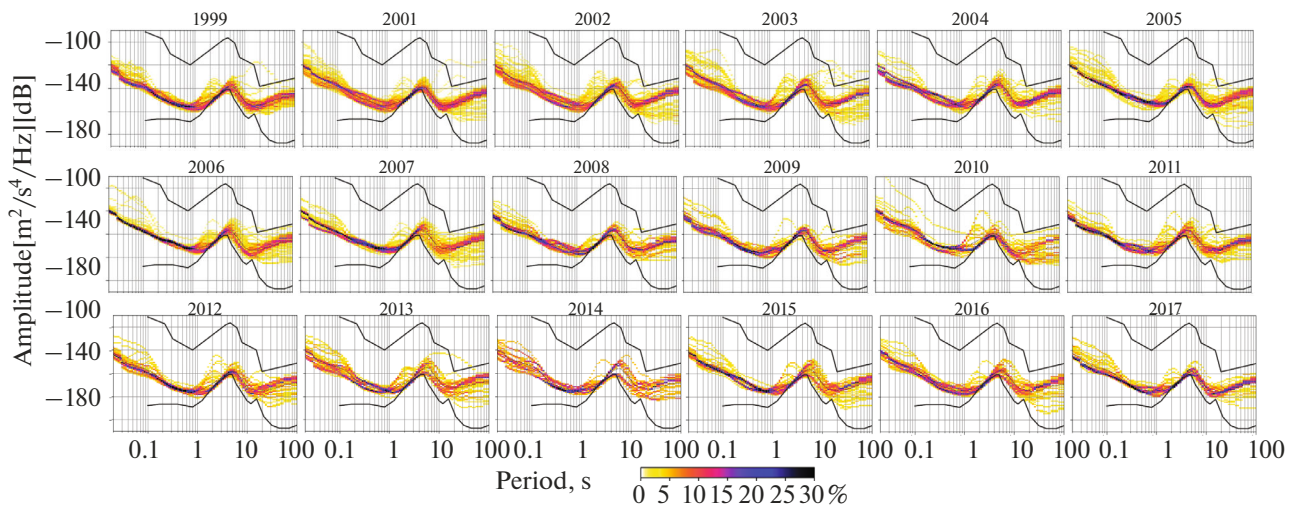


Fig. 9. The PPSD at the TKM2 station over years of study for the N channel.

component of seismic signals is excluded from consideration.

3. The lowest level of noise within various times of the day was observed around 00 and 18 hours UTC.

4. Noise level is affected by seasonal variations, with the largest departures occurring for longer periods (10–100 s) on the horizontal channels; the level at

periods of 5–10 s varies little over the seasons at all channels. The noise level at the above periods is lower in the summertime than in the winter. The AML, KZA, UCH, and KBK stations are the most sensitive to seasonal variations.

5. The noise level is nearly constant over the years at the KNET stations.

Table 10. The months of the years in which the level of seismic noise showed considerable deviations at some channels of the AML, KBK, KZA, and UCH stations

| Station | Month | E | N | Z |
|---------|-----------|--|--|---|
| AML | June | | 1999, 2001–2004, 2006–2007, 2010–2011, 2015–2017 | 1999, 2002–2003, 2006–2007, 2011, 2013, 2016–2017 |
| | September | | 2013, 2015 | 2015 |
| | December | 2005, 2007 | | 2005, 2007 |
| KBK | March | 1999, 2001–2002, 2005, 2007–2008, 2010, 2012, 2016 | 1999, 2002, 2005, 2007–2008, 2010, 2012, 2016 | 1999, 2002, 2005, 2007–2008, 2010, 2012, 2016 |
| | June | 2000–2003, 2005–2008, 2015 | 1999, 2001–2003, 2005–2008, 2015 | 1999, 2001–2002, 2015 |
| | September | 2002, 2006, 2009, 2012 | 2002, 2006, 2009, 2012 | 2002, 2006, 2009, 2012 |
| | December | 1999, 2002, 2004, 2010, 2011, 2013–2015 | 1999, 2002, 2013 | 1999, 2002 |
| KZA | September | 2003, 2005–2008, 2010–2011 | 2002–2003, 2005–2007, 2010, 2011 | 2001–2011, 2014 |
| | December | 2000, 2004, 2012 | 2000–2002, 2004, 2007, 2011–2012 | 2011–2013 |
| UCH | March | | 2009 | |
| | June | | 2009 | |
| | September | 2001–2002, 2007–2012, 2014, 2016 | 2001–2016 | 2001–2010, 2015, 2016 |
| | December | 2010, 2014, | 2007, 2010, 2012 | 2010, 2012, 2014 |

Grey cells mean that there is no substantial number of large deviations

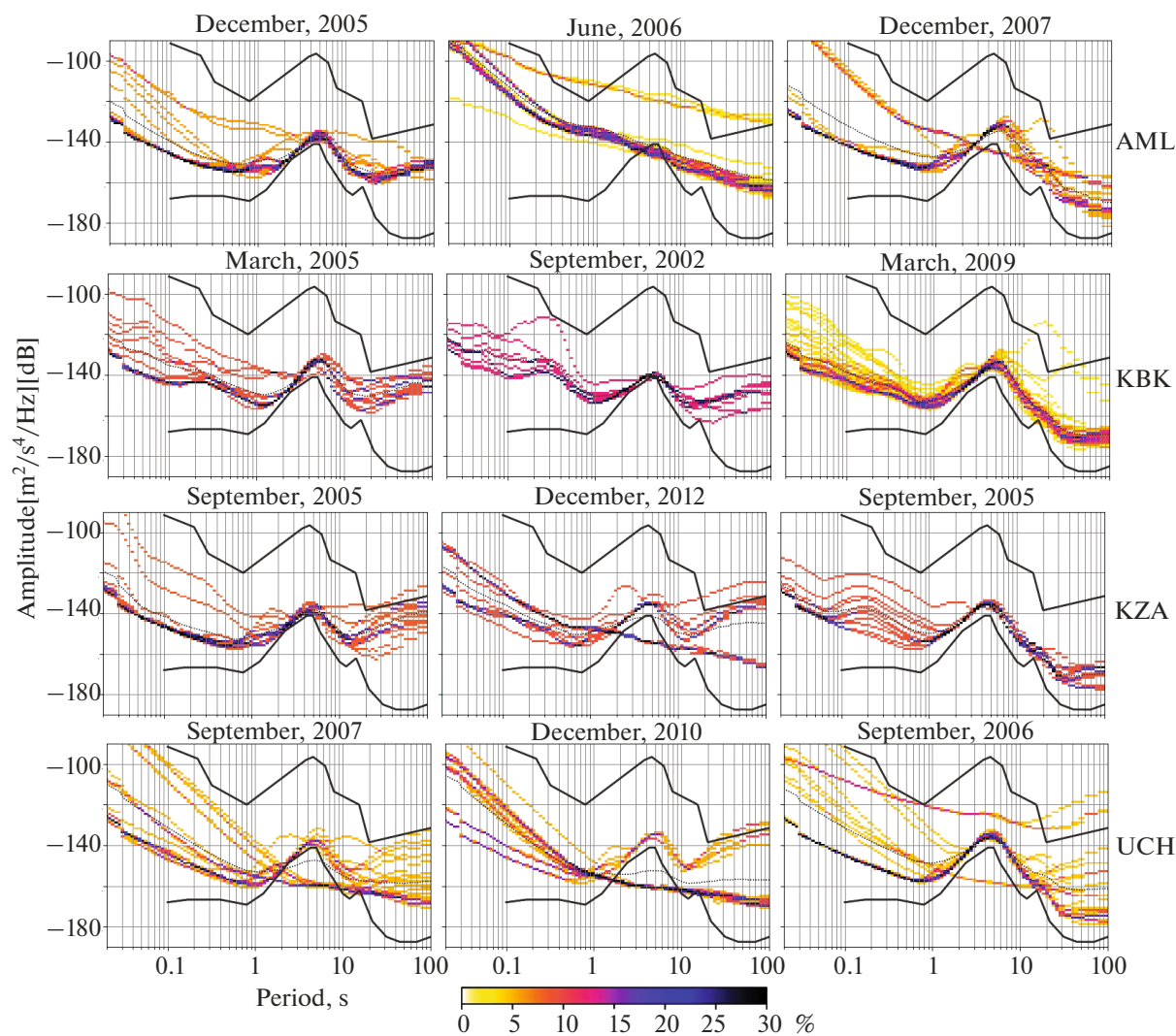


Fig. 10. The PPSD at the KNET stations during periods of unstable seismic noise.

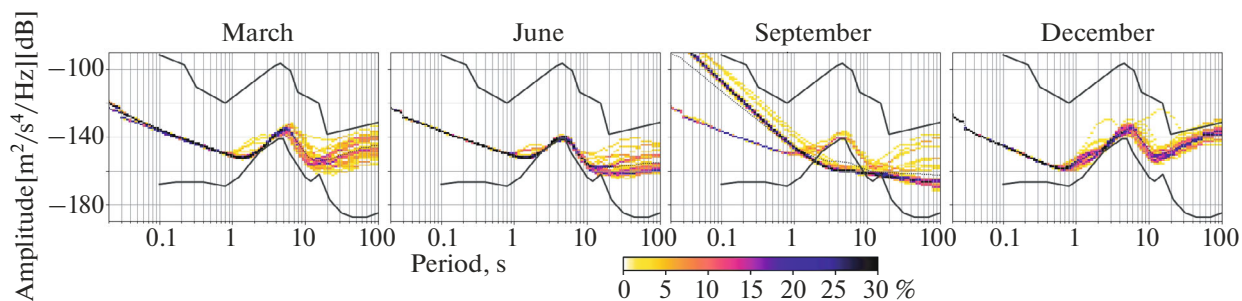


Fig. 11. The PPSD at the UCH station on the E channel for 2009.

An analysis of the noise PPSD at the KNET stations showed that the stations had satisfactory response functions, so that data from this network (continuous waveforms) can be used for studies that require low noise levels.

FUNDING

This study was supported in part by the state assignment of the Science Station of the Russian Academy of Sciences at Bishkek City according to the program of basic research IX.128, topic AAAA-A19-119020190066-3.

REFERENCES

- McNamara, D.E. and Buland, R.P., Ambient noise levels in the continental United States, *Bulletin of the Seismological Society of America*, 2004, vol. 94, no. 4, pp. 1517–1527.
<https://doi.org/10.1785/012003001>
- Nakamura, Y.A., Method for dynamic characteristics estimation of subsurface using microtremor on the ground surface, *QR Railw, Tech. Res. Inst.*, 1989, vol. 30, pp. 25–33.
- Peterson, J., Observation and modeling of seismic background noise, *U. S. Geol. Surv. Open-File Rept.*, 93–322, 1993, pp. 1–95.
- Sycheva, N.A., Bogomolov, L.M., and Sychev, V.N., On geoeffective solar flares and seismic noise variations, *Fizika Zemli*, 2011, no. 3, pp. 55–71.
- Sycheva, N.A. and Mansurov, A.N., Estimating station corrections for the KNET seismological network based on the analysis of the spectral ratio between the H and V components of seismic noise and local earthquakes, *Geofiz. Issledov.*, 2018, no. 19, pp. 30–48.
<https://doi.org/10.21455/gr2018.1-3>

Translated by A. Petrosyan